

## Antiferromagnetism of Ferrous Chloride Tetrahydrate $\text{FeCl}_2 \cdot 4\text{H}_2\text{O}$ †

NORIKIYO URYŪ\*

*Carnegie Institute of Technology, Pittsburgh, Pennsylvania*

(Received 29 April 1964)

The antiferromagnetism of the monoclinic crystal  $\text{FeCl}_2 \cdot 4\text{H}_2\text{O}$ , especially its ordered spin arrangement, is considered. By replacing the spin operators in the appropriate spin Hamiltonian by the classical spin vectors, we look for the lowest energy state of the spin arrangement. A model similar to one proposed by Spence *et al.* is obtained as the lowest energy arrangement of the spins, although it differs in detail. In doing so, we assume the four-sublattice model and isotropic exchange interactions between magnetic ions up to the fourth nearest neighbors. The susceptibilities in the directions of the magnetic principal axes are calculated at 0°K in a classical way. Comparison with the experimental results permits us to estimate the exchange integrals in reasonable order of magnitude.

### 1. INTRODUCTION

RECENT measurements of the specific heat, the susceptibility, the paramagnetic resonance absorption, and the proton resonance absorption in ferrous chloride tetrahydrate have revealed the details of the magnetic behavior at very low temperatures. Below about 1°K,  $\text{FeCl}_2 \cdot 4\text{H}_2\text{O}$  is in an antiferromagnetic state, and above about 1.5°K this crystal behaves as a typical paramagnetic salt like the Tutton salt or fluorosilicate.

A crystal of  $\text{FeCl}_2 \cdot 4\text{H}_2\text{O}$ , whose crystal growth habit was described by Groth,<sup>1</sup> belongs crystallographically to the monoclinic system. A detailed determination of the crystal structure has been made by Penfold and Grigor.<sup>2</sup> According to their results, its space group is  $P2_1/c$  and the dimensions of the unit cell are  $a=5.91$  Å,  $b=7.17$  Å (monoclinic or diad axis),  $c=8.44$  Å with  $\beta=112^\circ 10'$ .

The structure is made up of discrete units consisting of an  $\text{Fe}^{++}$  ion surrounded by two chlorine ions and four water molecules arranged in a distorted octahedron. In a unit cell, two of these groups are found, and  $\text{Fe}^{++}$  ions occupy inequivalent sites. In Fig. 1(a), the basic structural unit is shown. The O(1)-O(1) axis is perpendicular to the plane defined by the O(2)-O(2) and Cl-Cl axes, which make an angle of  $81^\circ$  with one another. Figure 1(b) indicates the relative orientations of the octahedra about the two inequivalent  $\text{Fe}^{++}$  ions in the unit cell. In this figure, we denote two inequivalent sites as A and B, and the two octahedra at both sites are projected on the  $z-x$  plane. The contents of a unit at site A may be transformed into those at site B by reflection in an  $a-c$  plane located at  $b/4$  followed by a translation of  $c/2$  along  $c$ . The two essentially parallel O(1)-O(1) axes at sites A and B lie very nearly in the  $a-c$  plane (tipping out of that plane by no more than  $1^\circ$ ) and deviate from the  $c$  direction by an angle of approximately  $3\frac{1}{2}^\circ$ . This local diad axis O(1)-O(1), which we call the microscopic  $z'$  axis, deviates from the principal susceptibility axis (which we call the macroscopic  $y$  axis) by no more

than  $2^\circ$ . The two sites A and B lie on two interpenetrating lattices and form a body-centered structure. That is, if we chose a B-site ion for the central ion the ions on the A site form a parallelepiped in which four rectangular faces are perpendicular to the  $a-c$  plane. The central ion has four nearest neighbors (n.n.) at 5.54 Å, two second n.n. in the  $a$  direction at 5.91 Å, four third n.n. at 6.84 Å and two fourth n.n. in the  $b$  direction at 7.71 Å.

Pierce and Friedberg<sup>3</sup> have measured the susceptibility of the powdered material and found that within the temperature range  $14\sim 20^\circ\text{K}$  the Curie-Weiss law  $\chi_m=3.61/(T+2)$  well describes its temperature dependence, and at about  $1.6^\circ\text{K}$  the susceptibility shows a maximum. Recently, within the temperature interval from 4.2 to  $0.35^\circ\text{K}$ , Schriempf and Friedberg<sup>4</sup> carried out single-crystal measurements along the  $b$ ,  $c$ , and  $a'$  axes, where the  $a'$  direction is perpendicular to both the  $b$  and  $c$  directions and lies in the  $a-c$  plane. Here we define the macroscopic axes  $x$ ,  $y$ , and  $z$  which take the place of  $a'$ ,  $c$ , and  $b$ , respectively. The most striking fact in the gross features of the measured susceptibility curves is that both  $\chi_b(\chi_z)$  and  $\chi_{a'}(\chi_x)$  pass through pronounced maxima at about  $1.5^\circ\text{K}$ , while  $\chi_c(\chi_y)$  is

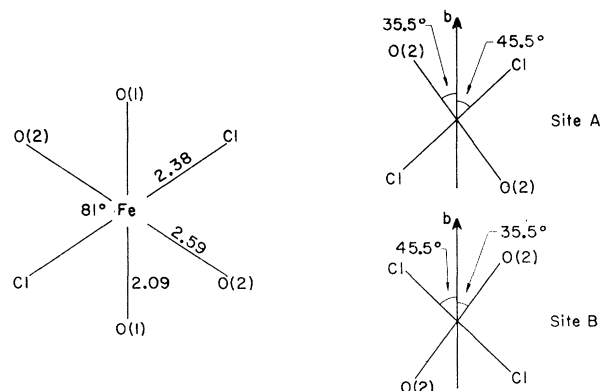


FIG. 1. (a) Local environment of  $\text{Fe}^{++}$  ion in the crystal of  $\text{FeCl}_2 \cdot 4\text{H}_2\text{O}$ . Unit of distance is angstroms. (b) Local environments of A- and B-site  $\text{Fe}^{++}$  ions projected on the  $z-x$  plane.

† Work supported by the National Science Foundation and the U. S. Office of Naval Research.

\* On leave from Department of Applied Science, Faculty of Engineering, Kyushu University, Fukuoka, Japan.

<sup>1</sup> P. Groth, *Chem. Kryst.* **1**, 246 (1906).

<sup>2</sup> B. R. Penfold and J. A. Grigor, *Acta Cryst.* **12**, 850 (1959).

<sup>3</sup> R. D. Pierce and S. A. Friedberg, *J. Appl. Phys.* **32**, 66S (1961).

<sup>4</sup> J. T. Schriempf and S. A. Friedberg (to be published).

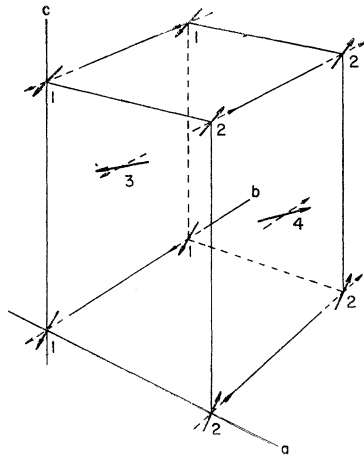


FIG. 2. The ordered spin arrangement in  $\text{FeCl}_2 \cdot 4\text{H}_2\text{O}$ . The dashed arrows show the spin arrangement proposed by Spence *et al.*, and the bold arrows show the one which has been obtained in the present work.

essentially temperature independent over much of the range stated. The location of the Néel temperature  $T_N$ , however, is near  $1^\circ\text{K}$  which corresponds to the temperature at which  $d\chi/dT$  assumes its maximum value. Specific heat measurements<sup>5</sup> also strongly suggest the occurrence of a cooperative transition near  $1^\circ\text{K}$ . Below  $T_N$ ,  $\chi_b(\chi_z)$  resembles the susceptibility of a typical antiferromagnet measured along the direction of preferred spin alignment, although there is some indication that the data taken at the lowest temperatures may extrapolate to a small finite value at  $0^\circ\text{K}$ .

Proton resonance studies by Spence *et al.*<sup>6</sup> suggest a curious transition phase lying between the paramagnetic and antiferromagnetic phases. Above  $1.1^\circ\text{K}$ , they observed a set of lines whose behavior with varying orientation indicates a paramagnetic state. At about  $1.1^\circ\text{K}$ , these lines disappear and no other lines are observed until the temperature is reduced to  $0.7^\circ\text{K}$ . Below  $0.7^\circ\text{K}$ , 16 lines whose angular dependence is characteristic of the antiferromagnetic state can be observed. This result should correspond to the fact that  $T_N$  will be located near  $1^\circ\text{K}$ . The 16 lines of the antiferromagnetic state arise from four different sets of local fields. Therefore, from symmetry considerations Spence *et al.* proposed the spin arrangement in the ordered state which is shown in Fig. 2.

Following the procedure employed by Schriempf and Friedberg, we first choose one of the microscopic principal axes of the crystalline field  $z'$  to coincide with the  $\text{O}(1)\text{-O}(1)$  direction. The other two local axes,  $y'$  and  $x'$ , are taken in the plane containing  $\text{O}(2)\text{-O}(2)$  and  $\text{Cl-Cl}$  pairs.  $x'$  makes an angle of  $\alpha$  with the  $b$  axis measured toward the appropriate  $\text{O}(2)\text{-O}(2)$  direction. Thus the macroscopic  $z$ - $x$  plane is essentially parallel to each  $x'$ - $y'$  plane. Here it should be noted that  $\alpha$  for the  $B$  ions has a different sign from the one for  $A$  ions.

As stated before, above  $1.5^\circ\text{K}$ ,  $\text{FeCl}_2 \cdot 4\text{H}_2\text{O}$  is a

<sup>5</sup> S. A. Friedberg, A. F. Cohen, and J. H. Schelleng, *J. Phys. Soc. Japan* **17**, Suppl. B-I, 515 (1962).

<sup>6</sup> R. D. Spence, R. Au, and P. Van Dalen, *Bull. Am. Phys. Soc.* **9**, 113 (1964).

typical paramagnetic salt, and we can well describe its magnetic behavior by the following spin Hamiltonian:

$$\mathcal{H} = D[S_z'^2 - \frac{1}{3}S(S+1)] + E(S_{x'}^2 - S_{y'}^2) + \mu_B(g_x H_x' S_x' + g_y H_y' S_y' + g_z H_z' S_z'), \quad (1.1)$$

where  $\mu_B$  the Bohr magneton,  $g_i$  the anisotropic splitting factor, and the crystalline field parameters  $D$  and  $E$  are defined as follows:

$$D = \lambda^2[\Lambda_{z'z'} - \frac{1}{2}(\Lambda_{x'x'} + \Lambda_{y'y'})], \quad (1.2a)$$

$$E = \frac{1}{2}\lambda^2[\Lambda_{x'x'} - \Lambda_{y'y'}], \quad (1.2b)$$

$$g_i = 2(1 - \lambda\Lambda_{ii}), \quad (1.2c)$$

and

$$\Lambda_{ij} = \sum_{n \neq 0} \langle 0 | L_i | n \rangle \langle n | L_j | 0 \rangle / (W_n - W_0). \quad (1.2d)$$

In these equations,  $\lambda$  is the spin-orbit coupling constant and  $W_n$  and  $|n\rangle$  are the  $n$ th energy level and the  $n$ th excited state, respectively, which are split from a degenerate  ${}^5D$  state of the free  $\text{Fe}^{2+}$  ion. In Eq. (1.1), the monoclinic symmetry of the microscopic crystalline field has been taken into account, and the weak exchange interactions between magnetic ions are tentatively neglected.

Starting from the spin Hamiltonian (1.1), we can calculate the paramagnetic susceptibilities in the directions of the microscopic principal axes as

$$\begin{aligned} \chi_{z'} &= \frac{2g_{z'}^2 \mu_B^2 / k}{T + (7/5)D + 2A^*}, \\ \chi_{x'} &= \frac{2g_{x'}^2 \mu_B^2 / k}{T - (7/10)(D - 3E) + 2A^*}, \\ \chi_{y'} &= \frac{2g_{y'}^2 \mu_B^2 / k}{T - (7/10)(D + 3E) + 2A^*}, \end{aligned} \quad (1.3)$$

where  $k$  is the Boltzmann constant and  $2A^*$  shows the additional term which will appear if we modify the Hamiltonian to include the effect of weak exchange interaction in a molecular-field approximation. We transform  $\chi_{x'}$ ,  $\chi_{y'}$ , and  $\chi_{z'}$  to the macroscopic principal susceptibilities  $\chi_x$ ,  $\chi_y$ , and  $\chi_z$  by the following relations.

$$\begin{aligned} \chi_{z'} &= \chi_y, \\ \chi_z &= \chi_{x'} \cos^2 \alpha + \chi_{y'} \sin^2 \alpha, \\ \chi_x &= \chi_{y'} \cos^2 \alpha + \chi_{x'} \sin^2 \alpha. \end{aligned} \quad (1.4)$$

By using the complete expressions for  $\chi_{x'}$ ,  $\chi_{y'}$ ,  $\chi_{z'}$  and (1.4), Schriempf and Friedberg have tried to get the values of  $D$ ,  $E$ , and  $\alpha$  which will give the best agreement with their measurements and have obtained

$$D = 1.83k, \quad E = -1.32k, \quad \alpha = 30^\circ. \quad (1.5)$$

The results (1.5) not only well explain both the magnetic and the thermal behavior of  $\text{FeCl}_2 \cdot 4\text{H}_2\text{O}$  in the paramagnetic region, but also will give us some information as to its antiferromagnetic state. In the next sec-

tion, we shall discuss the ordered spin arrangement in the antiferromagnetic state by using this result and a reasonable assumption about the exchange integrals which originate in the usual superexchange mechanism. Then we can get the lowest energy configuration of the spins. This configuration will be compared with the model proposed by Spence *et al.* We shall obtain an arrangement of the spins similar to that given by Spence *et al.*, but one in which the spins are canted in the  $x$ - $z$  plane and are not simply parallel to the  $b(z)$  axis. In Sec. 3, we calculate the susceptibilities at the absolute zero along three principal axes. The exchange parameters which appear in the susceptibility expression are estimated from the measured susceptibilities extrapolated to  $0^\circ\text{K}$ . In order to facilitate the mathematical manipulation, the above calculation does not include a contribution due to magnetic-dipole interaction, because its magnitude will be much smaller than the crystalline field effects. However, as we shall see, the estimated exchange parameters are found to be comparable in order of magnitude with the magnetic-dipole interaction. In the Appendix, its effects will be considered and discussed. Finally, in Sec. 4, we shall discuss the Moriya-Dzyaloshinsky<sup>7</sup> interactions which exist between first and third nearest neighbors.

## 2. ORDERED SPIN ARRANGEMENT

The fact that there are two inequivalent sites for  $\text{Fe}^{++}$  ions in a unit cell initially set us to considering a two-sublattice model in order to explain the antiferromagnetism. As stated in Sec. 1, the directions of the anisotropic crystalline fields around the  $A$ - and  $B$ -site ions are different from each other. Therefore, it may be possible to have the so-called parasitic ferromagnetism which is caused by canting the spins from pure antiparallelism.<sup>8,9</sup> Also, the Moriya-Dzyaloshinsky interaction will contribute to the canting and the parasitic ferromagnetism.  $\text{FeCl}_2 \cdot 4\text{H}_2\text{O}$ , however, does not exhibit any evidence of a spontaneous ferromagnetic moment at or below the Néel point. It appears, therefore, that a two-sublattice model is not realistic in this crystal.

As the next step, we shall take a four-sublattice model in which we further divide each sublattice of  $A$  or  $B$  ions into two sublattices. For this four-sublattice model, we want to seek the ordered spin arrangement in the antiferromagnetic state. In doing so, we assume that in each of the four sublattices all spins are parallel, and the spin operators which will appear in the Hamiltonian are replaced by classical vectors. In addition, the exchange interaction between spins are assumed to be isotropic. The exchange interactions will be taken up to fourth nearest neighbors.

The Hamiltonian for the present spin system can be

<sup>7</sup> I. Dzyaloshinsky, Phys. Chem. Solids 4, 241 (1958). T. Moriya, Phys. Rev. 120, 91 (1960).

<sup>8</sup> T. Oguchi, Busseiron Kenkyu (Japanese lang.) 93, 1 (1956). T. Moriya, Phys. Rev. 117, 635 (1960).

<sup>9</sup> N. Uryú, J. Phys. Soc. Japan 16, 2139 (1961).

written as

$$\mathcal{H} = \mathcal{H}_1 + \mathcal{H}_{\text{ex}}, \quad (2.1)$$

in which  $\mathcal{H}_1$  represents the sum of one-ion Hamiltonians (1.1) and  $\mathcal{H}_{\text{ex}}$  represents the exchange interactions. If we express  $\mathcal{H}_1$  in terms of spin components taken with respect to the macroscopic principal axes, we have

$$\begin{aligned} \mathcal{H}_1 = & \sum_{i=1,2} \{ D[S_y^{(i)2} - \frac{1}{3}S(S+1)] \\ & + A(S_x^{(i)2} - S_z^{(i)2}) + 2BS_x^{(i)}S_z^{(i)} \} \\ & + \sum_{i=3,4} \{ D[S_y^{(i)2} - \frac{1}{3}S(S+1)] \\ & + A(S_x^{(i)2} - S_z^{(i)2}) - 2BS_x^{(i)}S_z^{(i)} \}, \end{aligned} \quad (2.2)$$

where

$$A = -E \cos 2\alpha, \quad B = -E \sin 2\alpha, \quad (2.3)$$

and  $S_x^{(i)}$  shows the  $x$  component of the spin belonging to the  $i$ th sublattice, and so on. The exchange interaction can be written as

$$\mathcal{H}_{\text{ex}} = \sum_{\langle i,j \rangle} J_k \mathbf{S}_i \cdot \mathbf{S}_j, \quad (2.4)$$

in which the spin  $\mathbf{S}_j$  is the  $k$ th nearest-neighbor spin to the spin  $\mathbf{S}_i$  and the summation is taken all over the pairs of spins up to the fourth neighbors. We have four parameters  $J_k$  ( $k=1, 2, 3, 4$ ) which we assume to be isotropic exchange integrals between the spin  $\mathbf{S}_i$  and its  $k$ th nearest neighbor.

The combination of the sublattice spins appearing in  $\mathcal{H}_{\text{ex}}$  depends on the way in which we further divide the  $A$  and  $B$  ions into two sublattices. If we restrict the manner of division of  $A$  ( $B$ ) ions into two sublattices so as to have lattice points belonging to the same sublattice either uniquely or alternately along the crystal axes, there can be considered seven models as follows:

Type	Axis along which the sublattice points alternate
$G$	$a, b, c$
$\Gamma_1$	$a$
$\Gamma_2$	$b$
$\Gamma_3$	$c$
$\Gamma_1'$	$b, c$
$\Gamma_2'$	$a, c$
$\Gamma_3'$	$a, b$

We define the components of a vector  $\xi$  (in a twelve-dimensional space) by the components of the classical vectors  $\mathbf{S}^{(1)}$ ,  $\mathbf{S}^{(2)}$ ,  $\mathbf{S}^{(3)}$ , and  $\mathbf{S}^{(4)}$  as follows:

$$\begin{aligned} (\xi_1, \xi_2, \xi_3) &= (S_x^{(1)}, S_y^{(1)}, S_z^{(1)}), \\ (\xi_4, \xi_5, \xi_6) &= (S_x^{(2)}, S_y^{(2)}, S_z^{(2)}), \\ (\xi_7, \xi_8, \xi_9) &= (S_x^{(3)}, S_y^{(3)}, S_z^{(3)}), \\ (\xi_{10}, \xi_{11}, \xi_{12}) &= (S_x^{(4)}, S_y^{(4)}, S_z^{(4)}). \end{aligned} \quad (2.5)$$

Then, we can write  $4/N$  times the total energy in a form quadratic in  $\xi_i$  as

$$E = \sum A_{ij} \xi_i \xi_j \quad (A_{ij} = A_{ji}), \quad (2.6)$$



The matrix  $\mathbf{A}$  for  $\Gamma_2'$ , can be given in the identical form with that for  $\Gamma_2$  if we exchange  $J_2$  and  $J_4$ . In Eqs. (2.7),  $J$  and  $J'$  are defined as

$$J = J_1 + J_3, \quad J' = J_2 + J_4. \quad (2.8)$$

Following the method of Luttinger and Tisza,<sup>10</sup> the problem of finding the minimum value of (2.6) under a weak condition

$$\xi_1^2 + \xi_2^2 + \cdots + \xi_{12}^2 = \text{constant} \quad (2.9)$$

can be reduced to the diagonalization of the matrix  $\mathbf{A}$  for each type of four-sublattice arrangements. If the eigenvector belonging to the lowest eigenvalue obtained corresponds to a physically realistic solution, that is to say, if the solution satisfies also the strong conditions  $\xi_1^2 + \xi_2^2 + \xi_3^2 = \text{constant}$ , etc., that eigenvector should give the spin arrangement with the lowest energy among the possible four sublattice models.

To diagonalize each of these matrices, we transform it with the following orthogonal matrix

$$\mathbf{T} = \frac{1}{\sqrt{2}} \begin{pmatrix} 1 & 0 & 0 & 0 & 1 & 0 & 0 & 0 & 0 & 0 & 0 & 0 & 0 \\ 0 & 0 & 0 & 0 & 0 & 0 & 0 & 0 & 1 & 0 & 1 & 0 & 0 \\ 0 & 1 & 0 & 0 & 0 & 1 & 0 & 0 & 0 & 0 & 0 & 0 & 0 \\ 1 & 0 & 0 & 0 & -1 & 0 & 0 & 0 & 0 & 0 & 0 & 0 & 0 \\ 0 & 0 & 0 & 0 & 0 & 0 & 0 & 0 & 1 & 0 & -1 & 0 & 0 \\ 0 & 1 & 0 & 0 & 0 & -1 & 0 & 0 & 0 & 0 & 0 & 0 & 0 \\ 0 & 0 & 1 & 0 & 0 & 0 & 1 & 0 & 0 & 0 & 0 & 0 & 0 \\ 0 & 0 & 0 & 0 & 0 & 0 & 0 & 0 & 0 & 1 & 0 & 1 & 0 \\ 0 & 0 & 0 & 1 & 0 & 0 & 0 & 1 & 0 & 0 & 0 & 0 & 0 \\ 0 & 0 & 1 & 0 & 0 & 0 & -1 & 0 & 0 & 0 & 0 & 0 & 0 \\ 0 & 0 & 0 & 0 & 0 & 0 & 0 & 0 & 0 & 1 & 0 & -1 & 0 \\ 0 & 0 & 0 & 1 & 0 & 0 & 0 & -1 & 0 & 0 & 0 & 0 & 0 \end{pmatrix}. \quad (2.10)$$

Then Eqs. (2.7) are reduced, with respect to the new coordinate  $\xi' = \mathbf{T}\xi$ , to  $4 \times 4$  or  $2 \times 2$  submatrices, and the eigenvalues can be obtained as given in Table I.

Now, we want to compare the magnitudes of the twelve eigenvalues for each type of sublattice arrangement and to decide which is the smallest. Such a comparison seems to be not so easy, but the following facts or considerations will facilitate the task.

In  $\text{FeCl}_2 \cdot 4\text{H}_2\text{O}$ , the exchange interactions between  $\text{Fe}^{++}$  ions are of the superexchange type via at least two anions  $\text{O}_v^-$  or  $\text{Cl}^-$ . Examination of the detailed crystal structure given by Penfold and Grigor gives us some information about the superexchange mechanisms. Goodenough<sup>11</sup> and Kanamori<sup>12</sup> have classified the superexchange mechanisms for various cases of interacting cations. According to them,  $180^\circ$  interaction between  $d^6-d^6$  ions, each in an octahedral site, is antiferromagnetic if the relevant bond is a  $\sigma$  bond, and is weak (and of uncertain sign) if the relevant bond is a  $\pi$  bond. The present case is rather different, because there are

two intervening anions, and they are not in a line connecting two  $\text{Fe}^{++}$  ions. Consideration of the bond orbitals of the  $d$  and  $p$  electrons of the ions relevant to superexchange, however, permits us to assume

$$\begin{aligned} J_1, & \text{ small and uncertain in sign;} \\ J_2 > 0, & J_3 > 0 \text{ (antiferromagnetic);} \\ J_2 & \simeq J_3; \\ J_3 - J_1 & > 0; \\ J_4, & \text{ very small and possibly positive.} \end{aligned} \quad (2.11)$$

These assumptions permit us to select as the most stable spin configuration one whose susceptibilities are found to yield consistent  $J_k$ 's when fitted to the observed value. Further, we have from (1.5) and (2.3)

$$A = 0.66k, \quad B = 1.14k. \quad (2.12)$$

By using the assumption (2.11), and the fact  $A > 0$ ,  $B > 0$ , we can conclude the following:

$$\begin{aligned} (\epsilon_{\min})_G &= (\epsilon_{\min})_{\Gamma_3'} = -(J_2 + J_4) - \{A^2 + B^2\}^{1/2} \\ & \text{or} = J_2 + J_4 - [B^2 + \{A + 2(J_1 + J_3)\}^2]^{1/2}, \end{aligned} \quad (2.13)$$

<sup>10</sup> J. M. Luttinger and L. Tisza, Phys. Rev. **70**, 954 (1946). J. M. Luttinger, Phys. Rev. **81**, 1015 (1951).

<sup>11</sup> J. B. Goodenough, Phys. Chem. Solids, **6**, 287 (1958).

<sup>12</sup> J. Kanamori, Phys. Chem. Solids **10**, 87 (1959).

TABLE I. Eigenvalues of the matrix  $A$ .

Type			
$G, \Gamma_3'$	$\epsilon_1, \epsilon_2$	$D - J_2 - J_4$	
	$\epsilon_3$	$D + J_2 + J_4 \pm 2(J_1 + J_3)$	
	$\epsilon_4$		
	$\epsilon_5, \epsilon_7$	$-(J_2 + J_4) \pm \{A^2 + B^2\}^{1/2}$	
	$\epsilon_6, \epsilon_8$		
	$\epsilon_9$	$J_2 + J_4 + [B^2 + \{2(J_1 + J_3) \pm A\}^2]^{1/2}$	
	$\epsilon_{10}$		
	$\epsilon_{11}$	$J_2 + J_4 - [B^2 + \{2(J_1 + J_3) \pm A\}^2]^{1/2}$	
	$\epsilon_{12}$		
	$\Gamma_1$	$\epsilon_1$	$D + J_4 - J_2 \pm 2(J_1 - J_3)$
		$\epsilon_2$	
		$\epsilon_3$	$D + J_4 + J_2 \pm 2(J_1 + J_3)$
$\epsilon_4$			
$\epsilon_5$		$J_4 - J_2 + [B^2 + \{A \pm 2(J_1 - J_3)\}^2]^{1/2}$	
$\epsilon_6$			
$\epsilon_7$		$J_4 - J_2 - [B^2 + \{A \pm 2(J_1 - J_3)\}^2]^{1/2}$	
$\epsilon_8$			
$\epsilon_9$		$J_2 + J_4 + [B^2 + \{A \pm 2(J_1 + J_3)\}^2]^{1/2}$	
$\epsilon_{10}$			
$\epsilon_{11}$		$J_2 + J_4 - [B^2 + \{A \pm 2(J_1 + J_3)\}^2]^{1/2}$	
$\epsilon_{12}$			
$\Gamma_2, \Gamma_1'$	$\epsilon_1, \epsilon_2$	$D + J_2 - J_4$	
	$\epsilon_3$	$D + J_2 + J_4 \pm 2(J_1 + J_3)$	
	$\epsilon_4$		
	$\epsilon_5, \epsilon_7$	$J_2 - J_4 \pm \{B^2 + A^2\}^{1/2}$	
	$\epsilon_6, \epsilon_8$		
	$\epsilon_9$	$J_2 + J_4 + [B^2 + \{A \pm 2(J_1 + J_3)\}^2]^{1/2}$	
	$\epsilon_{10}$		
	$\epsilon_{11}$	$J_2 + J_4 - [B^2 + \{A \pm 2(J_1 + J_3)\}^2]^{1/2}$	
	$\epsilon_{12}$		
	$\Gamma_3$	$\epsilon_1, \epsilon_2$	$D + J_2 + J_4$
		$\epsilon_3$	$D + J_2 + J_4 \pm 2(J_1 + J_3)$
		$\epsilon_4$	
$\epsilon_5, \epsilon_7$		$J_2 + J_4 \pm \{A^2 + B^2\}^{1/2}$	
$\epsilon_6, \epsilon_8$			
$\epsilon_9$		$J_2 + J_4 + [B^2 + \{A \pm 2(J_1 + J_3)\}^2]^{1/2}$	
$\epsilon_{10}$			
$\epsilon_{11}$		$J_2 + J_4 - [B^2 + \{A \pm 2(J_1 + J_3)\}^2]^{1/2}$	
$\epsilon_{12}$			
$\Gamma_2'$		$\epsilon_1, \epsilon_2$	$D - J_2 + J_4$
		$\epsilon_3$	$D + J_2 + J_4 \pm 2(J_1 + J_3)$
		$\epsilon_4$	
	$\epsilon_5, \epsilon_7$	$-J_2 + J_4 \pm \{A^2 + B^2\}^{1/2}$	
	$\epsilon_6, \epsilon_8$		
	$\epsilon_9$	$J_2 + J_4 + [B^2 + \{A \pm 2(J_1 + J_3)\}^2]^{1/2}$	
	$\epsilon_{10}$		
	$\epsilon_{11}$	$J_2 + J_4 - [B^2 + \{A \pm 2(J_1 + J_3)\}^2]^{1/2}$	
	$\epsilon_{12}$		

$$(\epsilon_{\min})_{\Gamma_1} = J_2 + J_4 - [B^2 + \{A + 2(J_1 + J_3)\}^2]^{1/2},$$

$$\text{or } = -J_2 + J_4 - [B^2 + \{A + 2(J_3 - J_1)\}^2]^{1/2}, \quad (2.14)$$

$$(\epsilon_{\min})_{\Gamma_1} \leq (\epsilon_{\min})_{\Gamma_2'} \leq (\epsilon_{\min})_{\Gamma_2, \Gamma_1'} \leq (\epsilon_{\min})_{\Gamma_3}, \quad (2.15)$$

$$(\epsilon_{\min})_{G, \Gamma_3'} \leq (\epsilon_{\min})_{\Gamma_2'} \leq (\epsilon_{\min})_{\Gamma_2, \Gamma_1'} \leq (\epsilon_{\min})_{\Gamma_3}. \quad (2.16)$$

And further, if the inequality relation

$$J_2 > 2J_1\delta \quad (2.17)$$

with

$$\delta = (A + 2J_3) / \{B^2 + (A + 2J_3)^2\}^{1/2}, \quad 0 < \delta < 1 \quad (2.18)$$

is satisfied, we can conclude that the lowest eigenvalue belongs to type  $\Gamma_1$ , and

$$\epsilon_{\min} = -J_2 + J_4 - [B^2 + \{A + 2(J_3 - J_1)\}^2]^{1/2}. \quad (2.19)$$

The corresponding eigenvector is given by

$$\xi = 1/\sqrt{2}\{a, 0, b, -a, 0, -b, c, 0, d, -c, 0, -d\}, \quad (2.20)$$

where  $a, b, c$ , and  $d$  are determined by the following relations:

$$a^2 + b^2 + c^2 + d^2 = 1,$$

$$a + c = 0,$$

$$\frac{a}{b} = -\frac{c}{d} \quad (2.21)$$

$$= \frac{B}{A + 2(J_3 - J_1) + [B^2 + \{A + 2(J_3 - J_1)\}^2]^{1/2}}.$$

The latter two relations can be found easily from the  $4 \times 4$  submatrix of  $\mathbf{T}^{-1}\mathbf{A}\mathbf{T}$  ( $\mathbf{A}$  for type  $\Gamma_1$ ) in which the lowest eigenvalue (2.19) is included. This eigenvector is a physically realistic solution and the orientations of spins  $\mathbf{S}^{(1)}, \mathbf{S}^{(2)}, \mathbf{S}^{(3)}$ , and  $\mathbf{S}^{(4)}$  are found to be in the directions of the following four unit vectors, respectively,

$$\begin{aligned} \mathbf{S}^{(1)} &= \sqrt{2}\{a, 0, b\}, \\ \mathbf{S}^{(2)} &= \sqrt{2}\{-a, 0, -b\}, \\ \mathbf{S}^{(3)} &= \sqrt{2}\{-a, 0, b\}, \\ \mathbf{S}^{(4)} &= \sqrt{2}\{a, 0, -b\}. \end{aligned} \quad (2.22)$$

In Fig. 2 and Fig. 3, we show the arrangement of four sublattice spins. All spins make an angle  $\theta_0$  with the  $z$  axis in the  $z-x$  plane clockwise or counterclockwise, and  $\theta_0$  is given by

$$\theta_0 = \tan^{-1} \times \frac{B}{A + 2(J_3 - J_1) + [B^2 + \{A + 2(J_3 - J_1)\}^2]^{1/2}}. \quad (2.23)$$

In the sublattice type,  $\Gamma_1$ ,  $\mathbf{S}^{(1)}$  and  $\mathbf{S}^{(3)}$ , ( $\mathbf{S}^{(2)}$ , and  $\mathbf{S}^{(4)}$ ) are the spins in the same  $b-c$  plane. Therefore, if  $\theta_0 = 0$ , the present figure becomes identical with the spin arrangement shown in Fig. 2 by dashed arrows, in which, for instance,  $\mathbf{S}^{(1)}$  and  $\mathbf{S}^{(3)}$  point in the  $-z$  direction and  $\mathbf{S}^{(2)}$  and  $\mathbf{S}^{(4)}$  point in the  $+z$  direction. It should be pointed out that in the antiferromagnetic state there will exist  $x$  components of the spins, and the  $z$  axis is not the direction of the preferred spin alignment. Based on this spin arrangement, the small finite value of  $\chi_z$  extrapolated to  $0^\circ\text{K}$  can be explained, and the

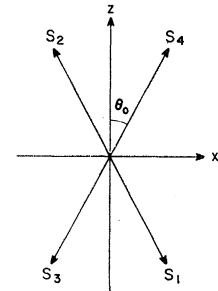


FIG. 3. The ordered spin arrangement of four sublattice spins.

explanation of the proton-resonance experiment should not be changed essentially.

### 3. SUSCEPTIBILITIES AT 0°K

As shown by the experiments of Schriempf and Friedberg,  $\chi_z$  resembles the susceptibility of a typical antiferromagnet measured along the direction of preferred spin alignment. The data taken at the lowest temperature, however, may extrapolate to a small finite value at 0°K. This corresponds to the fact that the  $z$  axis is not, strictly speaking, the preferred spin axis in the present four-sublattice model. Taking into account this situation, we shall calculate the susceptibilities along the directions of the principal axes at 0°K in the classical way.

Let us denote the direction cosines of the spins belonging to sublattice (1) by  $(\xi_0, 0, \zeta_0)$  in the absence of a magnet field. The direction cosines of the spins belonging to sublattices (2), (3), and (4) can be denoted by  $(-\xi_0, 0, -\zeta_0)$ ,  $(-\xi_0, 0, \zeta_0)$ , and  $(\xi_0, 0, -\zeta_0)$ , respectively. In the presence of a magnetic field, however, the direction cosines of these sublattice spins will be denoted as  $(\xi^{(1)}, \eta^{(1)}, \zeta^{(1)})$ ,  $(\xi^{(2)}, \eta^{(2)}, \zeta^{(2)})$ ,  $(\xi^{(3)}, \eta^{(3)}, \zeta^{(3)})$ , and  $(\xi^{(4)}, \eta^{(4)}, \zeta^{(4)})$ , respectively. If the polar and azimuthal angles corresponding to  $(\xi_0, 0, \zeta_0)$  and  $(\xi^{(1)}, \eta^{(1)}, \zeta^{(1)})$  are  $\pi/2 - \vartheta_0$  and 0, and  $\pi/2 - (\vartheta_0 + \theta_1)$  and  $\varphi_1$ , respectively, we have

$$\begin{aligned}\xi^{(1)} &= \cos(\vartheta_0 + \theta_1) \cos \varphi_1, \\ \eta^{(1)} &= \cos(\vartheta_0 + \theta_1) \sin \varphi_1, \\ \zeta^{(1)} &= \sin(\vartheta_0 + \theta_1).\end{aligned}\quad (3.1a)$$

Similarly,

$$\begin{aligned}\xi^{(2)} &= -\cos(\vartheta_0 + \theta_2) \cos \varphi_2, \\ \eta^{(2)} &= -\cos(\vartheta_0 + \theta_2) \sin \varphi_2, \\ \zeta^{(2)} &= -\sin(\vartheta_0 + \theta_2),\end{aligned}\quad (3.1b)$$

$$\begin{aligned}\xi^{(3)} &= -\cos(\vartheta_0 - \theta_3) \cos \varphi_3, \\ \eta^{(3)} &= -\cos(\vartheta_0 - \theta_3) \sin \varphi_3, \\ \zeta^{(3)} &= \sin(\vartheta_0 - \theta_3),\end{aligned}\quad (3.1c)$$

$$\begin{aligned}\xi^{(4)} &= \cos(-\vartheta_0 + \theta_4) \cos \varphi_4, \\ \eta^{(4)} &= \cos(-\vartheta_0 + \theta_4) \sin \varphi_4, \\ \zeta^{(4)} &= \sin(-\vartheta_0 + \theta_4).\end{aligned}\quad (3.1d)$$

We expand (3.1a) in powers of  $\theta_1$  and  $\varphi_1$  and have

$$\begin{aligned}\xi^{(1)} &= \xi_0 \left\{ 1 - \frac{1}{2}(\theta_1^2 + \varphi_1^2) \right\} - \zeta_0 \theta_1, \\ \eta^{(1)} &= \xi_0 \varphi_1 - \zeta_0 \theta_1 \varphi_1, \\ \zeta^{(1)} &= \zeta_0 \left( 1 - \frac{1}{2} \theta_1^2 \right) + \xi_0 \theta_1.\end{aligned}\quad (3.2)$$

Similar expressions for  $\xi^{(i)}$ ,  $\eta^{(i)}$ , and  $\zeta^{(i)}$  are obtained from (3.1b), (3.1c), and (3.1d).

We substitute these expressions into the energy expression (2.6) for the  $\Gamma_1$  type. Then terms linear with

respect to  $\varphi_1$ ,  $\varphi_2$ ,  $\varphi_3$ , and  $\varphi_4$  will not appear and terms linear with respect to  $\theta_1$ ,  $\theta_2$ ,  $\theta_3$ , and  $\theta_4$  will be seen to vanish, if we use the relation (2.23). Therefore, the energy up to quadratic terms can be written as

$$\begin{aligned}E &= (N/4)S^2 \{ E_0 + P(\theta_1^2 + \theta_2^2 + \theta_3^2 + \theta_4^2) - 4J_1(\xi_0^2 - \zeta_0^2) \\ &\quad \times (\theta_1\theta_3 + \theta_2\theta_4) - 2J_2(\theta_1\theta_2 + \theta_3\theta_4) \\ &\quad + 4J_3(\xi_0^2 - \zeta_0^2)(\theta_1\theta_4 + \theta_2\theta_3) + Q(\varphi_1^2 + \varphi_2^2 + \varphi_3^2 + \varphi_4^2) \\ &\quad - 4J_1\xi_0^2(\varphi_1\varphi_3 + \varphi_2\varphi_4) - 2J_2\xi_0^2(\varphi_1\varphi_2 + \varphi_3\varphi_4) \\ &\quad + 4J_3\xi_0^2(\varphi_1\varphi_4 + \varphi_2\varphi_3) \},\end{aligned}\quad (3.3)$$

where  $E_0$  and  $P$  and  $Q$  are given by

$$\begin{aligned}E_0 &= 4(J_4 - J_2) + 4(\xi_0^2 - \zeta_0^2)(A + 2J_3 - 2J_1) + 8B\xi_0\zeta_0, \\ P &= J_2 - 2(\xi_0^2 - \zeta_0^2)(A + J_3 - J_1) - 4B\xi_0\zeta_0, \\ Q &= (2J_1 + J_2 - 2J_3 + D - A)\xi_0^2 - B\xi_0\zeta_0.\end{aligned}\quad (3.4)$$

The magnetic moment along each coordinate axis can be expressed as

$$\begin{aligned}M_x &= (N/4)\mu_B S \{ g_1(\xi^{(1)} + \xi^{(2)} + \xi^{(3)} + \xi^{(4)}) \\ &\quad + g_4(\zeta^{(1)} + \zeta^{(2)} - \zeta^{(3)} - \zeta^{(4)}) \} \\ &= (N/4)\mu_B S \{ g_1(\xi_0/2)(-\theta_1^2 + \theta_2^2 + \theta_3^2 - \theta_4^2) \\ &\quad + g_1\zeta_0(-\theta_1 + \theta_2 - \theta_3 + \theta_4) \\ &\quad + g_4(\zeta_0/2)(-\theta_1^2 + \theta_2^2 + \theta_3^2 - \theta_4^2) \\ &\quad + g_4\xi_0(\theta_1 - \theta_2 + \theta_3 - \theta_4) \},\end{aligned}\quad (3.5a)$$

$$\begin{aligned}M_y &= (N/4)\mu_B S g_2(\eta^{(1)} + \eta^{(2)} + \eta^{(3)} + \eta^{(4)}) \\ &= (N/4)\mu_B S g_2 \{ \xi_0(\varphi_1 - \varphi_2 - \varphi_3 + \varphi_4) \\ &\quad - \zeta_0(\theta_1\varphi_1 - \theta_2\varphi_2 + \theta_3\varphi_3 - \theta_4\varphi_4) \},\end{aligned}\quad (3.5b)$$

$$\begin{aligned}M_z &= (N/4)\mu_B S \{ g_3(\zeta^{(1)} + \zeta^{(2)} + \zeta^{(3)} + \zeta^{(4)}) \\ &\quad + g_4(\xi^{(1)} + \xi^{(2)} - \xi^{(3)} - \xi^{(4)}) \} \\ &= (N/4)\mu_B S \{ g_3(\zeta_0/2)(-\theta_1^2 + \theta_2^2 - \theta_3^2 + \theta_4^2) \\ &\quad + g_3\xi_0(\theta_1 - \theta_2 - \theta_3 + \theta_4) \\ &\quad + g_4(\xi_0/2)(-\theta_1^2 + \theta_2^2 - \theta_3^2 + \theta_4^2) \\ &\quad + g_4\zeta_0(-\theta_1 + \theta_2 + \theta_3 - \theta_4) \},\end{aligned}\quad (3.5c)$$

where  $g_1$ ,  $g_2$ ,  $g_3$ , and  $g_4$  are the nonzero components of the single-ion  $g$  tensor in the system of macroscopic principal axes and are given by

$$\begin{aligned}g_1 &= g_{xx} = g_{y'} \cos^2 \alpha + g_{x'} \sin^2 \alpha, \\ g_2 &= g_{yy} = g_{z'}, \\ g_3 &= g_{zz} = g_{y'} \sin^2 \alpha + g_{x'} \cos^2 \alpha, \\ g_4 &= g_{xz} = (g_{y'} - g_{x'}) \sin \alpha \cos \alpha.\end{aligned}\quad (3.6)$$

For ions of sublattices (3) and (4),  $g_4$  has the opposite sign. The spin orientation of lowest energy in the presence of a magnetic field  $\mathbf{H}$  can be obtained by minimizing  $E - \mathbf{M} \cdot \mathbf{H}$  with respect to  $\theta_i$  and  $\varphi_i$ . The values of  $\theta_i$  and  $\varphi_i$  which correspond to that spin orientation are substituted in the expression for the magnetic moment, and so the susceptibility  $\chi_i$  will be obtained.

First in the case of  $\mathbf{H} \parallel x$  axis. The minimization of

$E-M_xH$  leads to

$$\varphi_1 = \varphi_2 = \varphi_3 = \varphi_4 = 0, \quad (3.7)$$

$$\theta_1 = -\theta_4 = (-1/\Delta)(\sigma_1\xi_0 - \sigma_4\xi_0) \times \{2P - \sigma_1\xi_0 - \sigma_4\xi_0 - 4J_3(\xi_0^2 - \zeta_0^2) - 2J_2 + 4J_1(\xi_0^2 - \zeta_0^2)\}, \quad (3.8)$$

$$\theta_2 = -\theta_3 = (1/\Delta)(\sigma_1\xi_0 - \sigma_4\xi_0) \times \{2P + \sigma_1\xi_0 + \sigma_4\xi_0 - 4J_3(\xi_0^2 - \zeta_0^2) - 2J_2 + 4J_1(\xi_0^2 - \zeta_0^2)\}, \quad (3.9)$$

where

$$\Delta = \{2P - 4J_3(\xi_0^2 - \zeta_0^2)\}^2 - (\sigma_1\xi_0 + \sigma_4\xi_0)^2 - \{2J_2 - 4J_1(\xi_0^2 - \zeta_0^2)\}^2, \quad (3.10)$$

$$\sigma_i = \mu_B H g_i / S. \quad (3.11)$$

The susceptibility along the  $x$  axis  $\chi_x$  can therefore be written as

$$\chi_x = \frac{N\mu_B^2(g_1\xi_0 - g_4\xi_0)^2}{4J_2 - 4(\xi_0^2 - \zeta_0^2)(A + 2J_3) - 8B\xi_0\xi_0} = \frac{N\mu_B^2g_1^2}{8} \left\{ 1 + \frac{g_4}{g_1} \frac{B}{K + (B^2 + K^2)^{1/2}} \right\}^2 \times \frac{(B^2 + K^2)^{1/2} + K}{J_2(B^2 + K^2)^{1/2} + K(A + 2J_3) + B^2}, \quad (3.12)$$

where

$$K = A + 2(J_3 - J_1). \quad (3.13)$$

Let us next calculate  $\chi_z$ . In this case, we have a solution

$$\varphi_1 = \varphi_2 = \varphi_3 = \varphi_4 = 0, \quad (3.14)$$

$$\theta_1 = -\theta_3 = (1/\Delta')(\sigma_3\xi_0 - \sigma_4\xi_0) \times \{2P - \sigma_3\xi_0 - \sigma_4\xi_0 + 4J_1(\xi_0^2 - \zeta_0^2) - 2J_2 - 4J_3(\xi_0^2 - \zeta_0^2)\}, \quad (3.15)$$

$$\theta_2 = -\theta_4 = (-1/\Delta')(\sigma_3\xi_0 - \sigma_4\xi_0) \times \{2P + \sigma_3\xi_0 + \sigma_4\xi_0 + 4J_1(\xi_0^2 - \zeta_0^2) - 2J_2 - 4J_3(\xi_0^2 - \zeta_0^2)\}, \quad (3.16)$$

where

$$\Delta' = \{2P + 4J_1(\xi_0^2 - \zeta_0^2)\}^2 - (\sigma_3\xi_0 + \sigma_4\xi_0)^2 - \{2J_2 + 4J_3(\xi_0^2 - \zeta_0^2)\}^2. \quad (3.17)$$

So we have

$$\chi_z = \frac{N\mu_B^2(g_3\xi_0 - g_4\xi_0)^2}{4J_2 + 4(\xi_0^2 - \zeta_0^2)(2J_1 - A) - 8B\xi_0\xi_0} = \frac{N\mu_B^2g_3^2}{8} \left\{ 1 + \frac{g_4}{g_3} \frac{K + (B^2 + K^2)^{1/2}}{B} \right\}^2 \times \frac{(B^2 + K^2)^{1/2} - K}{J_2(B^2 + K^2)^{1/2} + K(A - 2J_1) + B^2}. \quad (3.18)$$

Finally, to obtain  $\chi_y$  in the presence of a magnetic field along the  $y$  axis, we note that there is a solution

$$\theta_1 = \theta_2 = -\theta_3 = -\theta_4 = -\sigma_2\xi_0\varphi_1 / \{2P - 2J_2 + 4(\xi_0^2 - \zeta_0^2)(J_1 - J_3)\}, \quad (3.19)$$

$$\varphi_1 = -\varphi_2 = -\varphi_3 = \varphi_4 = \frac{\sigma_2\xi_0\{2P - 2J_2 + 4(\xi_0^2 - \zeta_0^2)(J_1 - J_3)\}}{\{2Q + 2\xi_0^2(J_2 + 2J_1 + 2J_3)\}\{2P - 2J_2 + 4(\xi_0^2 - \zeta_0^2)(J_1 - J_3)\} - (\sigma_2\xi_0)^2}. \quad (3.20)$$

Thus the susceptibility is written as

$$\chi_y = \frac{N\mu_B^2g_2^2}{2} \frac{\xi_0^2}{(4J_1 + 2J_2 + D - A)\xi_0^2 - B\xi_0\xi_0}, = \frac{N\mu_B^2g_2^2}{2} \frac{1}{2(J_1 + J_2 + J_3) + D + (B^2 + K^2)^{1/2}}. \quad (3.21)$$

The susceptibilities  $\chi_x$ ,  $\chi_y$ , and  $\chi_z$  which are given by Eqs. (3.12), (3.21), and (3.18), respectively, will be compared with the experimental values extrapolated to 0°K. Within the limits of experimental uncertainty, these may be taken to be

$$\begin{aligned} \chi_x &= 0.24 \text{ (cgs/mole),} \\ \chi_y &= 0.26, \\ \chi_z &= 0.07. \end{aligned} \quad (3.22)$$

According to Schriempf and Friedberg, the calculated splitting factors are approximately  $g_x = 2.16$ ,  $g_y = 2.20$ , and  $g_z = 2.21$ . Then we have, from (3.6),

$$g_1 = 2.20, \quad g_2 = 2.21, \quad g_3 = 2.18, \quad g_4 = 0.02. \quad (3.23)$$

The exchange parameters  $J_1$ ,  $J_2$ , and  $J_3$  can then be estimated by using these numerical values. First, we can eliminate  $J_2$  from two equations [(3.12) and (3.18)] and get a relation

$$J_3 + J_1 = F_1(J_3 - J_1). \quad (3.24)$$

Similarly, after some manipulation, we can get another relation

$$J_3 + J_1 = F_2(J_3 - J_1) \quad (3.25)$$

from (3.12) and (3.21). These are plotted in Fig. 4. Both curves cross only at  $J_3 - J_1 = 0.055k$  and  $J_3 + J_1 = 0.040k$ .



Thus we obtain

$$J_1 = -0.007k, \quad J_3 = 0.047k,$$

and by substituting them into (3.21), we get

$$J_2 = 0.103k.$$

These estimations seem to be reasonable in their order of magnitude and are consistent with the assumption (2.11). By using these values, we have  $\delta = 0.55$ . This is also consistent with the assumed inequality relation (2.17). Therefore, our four sublattice model will explain the antiferromagnetism in  $\text{FeCl}_2 \cdot 4\text{H}_2\text{O}$  satisfactorily with the above exchange integrals. The angle  $\theta_0$  that the spin axis makes with the  $z$  axis amounts to  $28^\circ$ .

#### 4. DISCUSSION

The spin arrangement in  $\text{FeCl}_2 \cdot 4\text{H}_2\text{O}$  which we obtain using a four-sublattice model is analogous to that in  $\text{CuCl}_2 \cdot 2\text{H}_2\text{O}$ . Moriya has proposed a spin arrangement in antiferromagnetic  $\text{CuCl}_2 \cdot 2\text{H}_2\text{O}$  in which spins alternately deviate from the preferred spin axis ( $a$  axis) clockwise or counterclockwise in the  $a$ - $c$  plane. In  $\text{CuCl}_2 \cdot 2\text{H}_2\text{O}$ , the so-called Moriya-Dzyaloshinsky interaction  $\mathbf{D} \cdot (\mathbf{S}_1 \times \mathbf{S}_2)$  exists between two spins  $\mathbf{S}_1$  and  $\mathbf{S}_2$  in addition to the ordinary exchange interaction and gives rise to a deviation from the pure antiparallelism of two spins.

Let us designate the point bisecting the straight line which connects two ions as  $C$ . We can see that in  $\text{FeCl}_2 \cdot 4\text{H}_2\text{O}$ ,  $\mathbf{D}$  for the first nearest-neighboring ions should be parallel to the  $c$  axis because there exists along the  $b$  direction a screw axis through the point  $C$  (so that  $\mathbf{D} \perp b$  axis) and an approximate twofold axis exists at  $C$  along the  $a'$  axis (so that  $\mathbf{D} \perp a'$  axis).  $\mathbf{D}$  for the second or the fourth nearest-neighboring ions should be zero, because a center of inversion is located at  $C$  in both cases. Between third nearest-neighbor ions,  $\mathbf{D}$  also exists ( $\mathbf{D} \perp b$  axis). According to Moriya,  $|\mathbf{D}| \cong (\Delta g/g)J$  where  $\Delta g$  is the deviation of the  $g$  factor from the value for a free electron. In the present case, it amounts to about 10% of  $J$ . Due to this interaction, the angle  $\theta_0$  of  $28^\circ$  in the  $z$ - $x$  plane might be slightly changed. Our present pattern of spin arrangement could be considered to originate mainly in the one-ion anisotropic crystalline field, as can be seen from its derivation. Because  $J_1$  and  $J_3$  are small compared with the coefficient of the crystalline field, the Moriya-Dzyaloshinsky contributions are not expected to modify the present results significantly.

In the molecular field approximation, the Néel temperature  $T_N$  is given by the highest root of the simultaneous equations relating the components of the spin vectors. It becomes clear that the roots of such an equation are equal to the eigenvalues of (2.7b) reversed in sign and with a factor  $2S(S+1)/3k$ . Therefore, the Néel temperature is given by

$$T_N = \{2S(S+1)/3k\} \times [J_2 - J_4 + [B^2 + \{A + 2(J_3 - J_1)\}^2]^{1/2}].$$

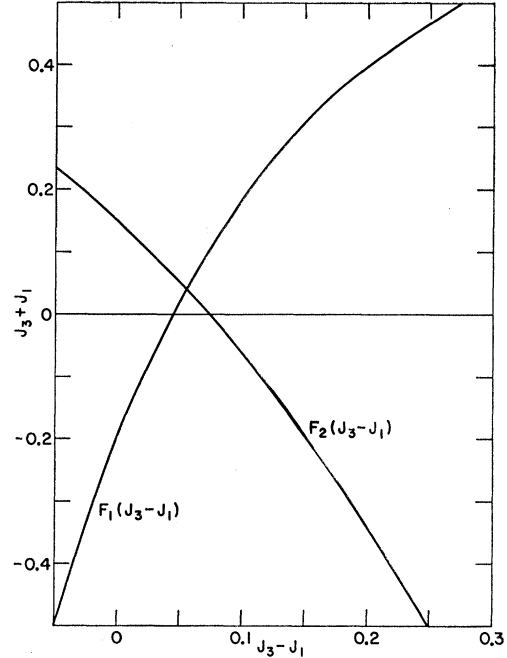


FIG. 4. Dependence of functions  $F_1(J_3 - J_1)$  and  $F_2(J_3 - J_1)$  upon  $J_3 - J_1$ .  $F_2(J_3 - J_1)$  is monotonic, whereas  $F_1(J_3 - J_1)$  should diverge to infinity at  $J_3 - J_1 = -A/2$ . Both curves, however, cross only once at the point shown in this figure. The coordinates are in unit of  $k$ .

Taking  $S = 2$ , and using the estimates of the isotropic exchange parameters, we get  $T_N = 5.92^\circ\text{K}$ . As there is no estimate of  $J_4$ , we put  $J_4 = 0$  to get this value of  $T_N$ . This will be too large even though we started from the molecular-field approximation. The low-lying two levels of the spin quintet which are separated more than  $8k$  from the excited levels and whose separation is about  $0.1k$  would suggest to us a fictitious spin of one-half in the antiferromagnetic state. If so, we can evaluate  $T_N = 0.74^\circ\text{K}$ , which is reasonably consistent with the value deduced from the magnetic measurements.

#### ACKNOWLEDGMENTS

The author would like to express his sincere thanks to Professor S. A. Friedberg for helpful discussions during the course of this work. The author is also grateful for the hospitality of the staff of the Physics Department, Carnegie Institute of Technology.

#### APPENDIX

The effect of the dipole interaction on the results which we have obtained in the text will be considered here. The dipole interaction is given, as usual,

$$\mathcal{H}_{\text{dip}} = \sum_{i>k} r_{ik}^{-3} [\mathbf{u}_i \cdot \mathbf{u}_k - 3(\mathbf{u}_i \cdot \mathbf{t}_{ik})(\mathbf{u}_k \cdot \mathbf{t}_{ik})], \quad (\text{A1})$$

where  $\mathbf{t}_{ik}$  is the unit vector connecting the ions  $i$  and  $k$   $r_{ik}$  the distance between them, and  $\mathbf{u}_i = \mathbf{g}_{\mu\text{B}} \mathbf{S}_i$  the mag

TABLE II. Numerical values of  $G_r^\mu$  (in units of  $\text{cm}^{-3}$ ).

$\mu$	$G_1^\mu \times 10^{-22}$	$G_2^\mu \times 10^{-22}$	$G_3^\mu \times 10^{-22}$	$G_4^\mu \times 10^{-22}$
$x$	2.237	-1.455	-0.869	0.740
$y$	-1.648	0.467	0.552	-0.126
$z$	-0.588	0.989	0.318	-0.614

netic moment. For the dipole and exchange interactions, the Hamiltonian of the  $l$ th spin can be written as

$$\mathfrak{H}_{\text{dip}} + \mathfrak{H}_{\text{ex}} = \sum_{m\nu} C_{\mu\nu}^{(lm)} S_{l\mu} S_{m\nu}, \quad (\text{A2})$$

where suffixes  $\mu$  and  $\nu$  represent coordinates  $x$ ,  $y$ , and  $z$ .

Due to the crystalline symmetry,  $\sum_m C_{xz}^{(lm)}$  and  $\sum_m C_{yz}^{(lm)}$  will vanish, and the nonzero coefficients can be obtained using the dipole sum and the exchange parameters. This can be done in the same way as in the author's previous work on the Tutton salts.<sup>9</sup> As we are considering the four-sublattice model, summation is taken over lattice points belonging to each sublattice. We have to consider seven sublattice models as in Sec. 2, and so the nonzero coefficients  $\sum_m C_{xx}^{(lm)}$ , etc., have different values depending on the model. The matrices corresponding to Eqs. (2.7) become very complicated, and the corresponding eigenvalue problems cannot be solved analytically. However, as to the effect of the dipole interaction on the ordered spin arrangement, we can make the following statements: In the present spin system, the dominant energy is the interaction with the crystalline field (2.2). The ordered spin arrangement in which spin components are mostly in the  $z$  direction can be easily understood because  $A$  and  $D$  have positive values. We shall consider the dipole energy in the case in which all spins are along the  $z$  axis. Then we can conclude that the most stable arrangement is one in which spins in one  $b$ - $c$  plane are parallel to one another and antiparallel to those in adjacent  $b$ - $c$  plane. There is no conflict with the previous conclusion that the lowest energy spin arrangement is of the  $\Gamma_1$  type. Because of the monoclinic crystal symmetry we have the nonvanishing  $xy$  component  $\sum_m C_{xy}^{(lm)}$ . Therefore, strictly speaking, the dipole interaction not only slightly changes the spin orientation in the  $x$ - $z$  plane, but also gives rise to a deviation from the  $x$ - $z$  plane, though it may be very small.

Next we shall modify the calculation of the susceptibilities in Sec. 3. For simplicity, we shall neglect  $g_4$  in  $\mathfrak{H}_{\text{dip}}$  and define the following dipole sums.

$$\begin{aligned} G_1^\mu &= \sum_k^{(3)} [1 - 3(t_{ik}^\mu)^2] / r_{ik}^3, \\ G_2^\mu &= \sum_k^{(2)} [1 - 3(t_{ik}^\mu)^2] / r_{ik}^3, \\ G_3^\mu &= \sum_k^{(4)} [1 - 3(t_{ik}^\mu)^2] / r_{ik}^3, \\ G_4^\mu &= \sum_k^{(1)} [1 - 3(t_{ik}^\mu)^2] / r_{ik}^3, \end{aligned} \quad (\text{A3})$$

where  $t_{ik}^\mu$  is the  $\mu$  component ( $\mu = x, y, z$ ) of  $\mathbf{t}_{ik}$ , and the lattice point  $i$  is on the sublattice (1), and  $\sum_k^{(j)}$  means the summation over the lattice points of the  $j$ th sublattice. The numerical values for the  $\Gamma_1$  type are listed in Table II.

The modified expressions for  $\chi_x$ ,  $\chi_y$ , and  $\chi_z$  are given as follows:

$$\begin{aligned} \chi_x &= N\mu_B^2 (g_1 \zeta_0 - g_4 \xi_0)^2 \{4J_2 - 4(\xi_0^2 - \zeta_0^2)(A + 2J_3) \\ &\quad - 8B\xi_0 \zeta_0 + 4(G_1^x - G_1^z) + 2(G_2^x + G_2^z) \\ &\quad - 4(G_3^x + G_3^z)(\xi_0^2 - \zeta_0^2) \\ &\quad + 2(G_4^z - G_4^x)(\xi_0^2 - \zeta_0^2)\}^{-1}, \end{aligned} \quad (\text{A4})$$

$$\begin{aligned} \chi_y &= (N\mu_B^2 g^2 \xi_0^2 / 2) \{ (4J_1 + 2J_2 + D - A)\xi_0^2 - B\xi_0 \zeta_0 \\ &\quad + [2(G_1^x + G_1^y) + (G_2^x + G_2^y) - 2(G_3^x - G_3^y) \\ &\quad - (G_4^x - G_4^y)]\xi_0^2 \}^{-1}, \end{aligned} \quad (\text{A5})$$

$$\begin{aligned} \chi_z &= N\mu_B^2 (g_3 \xi_0 - g_4 \zeta_0)^2 \{4J_2 + 4(\xi_0^2 - \zeta_0^2)(2J_1 - A) \\ &\quad - 8B\xi_0 \zeta_0 + 4(G_1^x + G_1^z)(\xi_0^2 - \zeta_0^2) \\ &\quad + 2(G_2^x + G_2^z) - 4(G_3^x - G_3^z) \\ &\quad + 2(G_4^z - G_4^x)(\xi_0^2 - \zeta_0^2)\}^{-1}. \end{aligned} \quad (\text{A6})$$

Accordingly, the two curves of Eqs. (3.24) and (3.25) shown in Fig. 4 would shift and cross at another point, namely,  $J_3 - J_1 = 0.080k$  and  $J_3 + J_1 = 0.070k$ . Therefore our previous estimates of the exchange parameters would be changed to

$$J_1 = -0.005k, \quad J_2 = 0.154k, \quad J_3 = 0.075k.$$

These values are still consistent with the assumption (2.11) and (2.17) and seem to be reasonable in their order of magnitude. The corrected value of the angle  $\theta_0$  is  $27^\circ$ .